

# The ball on three balls test for strength testing of brittle discs: Part II: analysis of possible errors in the strength determination

Andreas Börger<sup>a,\*</sup>, Peter Supancic<sup>a,b</sup>, Robert Danzer<sup>a,b</sup>

<sup>a</sup>*Department for Structural and Functional Ceramics, University of Leoben, A-8700 Leoben, Austria*

<sup>b</sup>*Materials Center Leoben, A-8700 Leoben, Austria*

Received 12 July 2003; received in revised form 2 October 2003; accepted 16 October 2003

## Abstract

Biaxial strength testing of brittle materials using the ball on three balls test (B3B test) is a useful tool for direct strength testing of disc specimens offering some advantages compared with the testing of bended beams: there are less problems with the alignment of the specimens in the fixture, in many cases the production of the specimens is easier, the area of maximum tensile stress amplitudes is far from the edges of the specimen (were often machining defects exist) and the testing procedure can easier be miniaturised. In a preceding paper, a proposal for a suitable testing set up was made, the stress fields in the disc specimens were analysed and first testing results were reported. A simple solution for the maximum tensile stress amplitude in the discs was given for a range of parameters concerning the geometry of the specimen, the supporting situation during the test and the material properties. In this paper, possible sources for deviations of this stress from the reported idealised solution (which would result in measuring errors) are discussed. For example, the not accounted influence of friction forces between the disc and the support balls, the influence of a possible buckling of the disc and the influence of geometric inaccuracies are analysed. It is shown, that the thickness of the disc is the most sensitive parameter determining the maximum tensile stress. Therefore it has to be determined with high accuracy.

© 2003 Elsevier Ltd. All rights reserved.

**Keywords:** Ball on three balls; Mechanical properties; Strength; Testing

## 1. Introduction

Biaxial strength testing of brittle materials has some advantages compared to uni-axial bending testing, which are described in the literature (see also citations in Ref. 1, where a more extensive review on the literature is given). For example the easier test piece preparation, the testing of a large surface area free from edge finishing defects or the more relevant testing situation for many components are claimed. Biaxial strength testing has been used for many years and there exists a wide variety of test assemblies described in the literature.<sup>1,2</sup> The support of the specimens is either realised by a ring or by three or more balls (a ring of balls) and the loading by a ring, a ball or a punch resulting in axi-symmetric and non axi-symmetric loading situations.

In the case of the axi-symmetric loading situations the stress field in the disc specimens can be determined

relatively easily but in reality, small inaccuracies from the idealised geometry of specimen, support and loading will break the symmetry and can cause large deviations from the idealised solutions. In the case of non axi-symmetric loading situations the determination of the stress field in the specimen is difficult and can only be done properly using numerical methods. Such a systematic investigation could not be found in the literature before.<sup>1</sup>

In the preceding paper,<sup>1</sup> the stress fields in the specimens loaded in the ball on three balls tests (B3B-test) were analysed. The investigated set-up of the B3B-testing geometry is shown in Fig. 1. To reduce the number of parameters it was assumed that the loading ball is of the same size as the support balls. The support balls are of equal size and touch each other. This leads to a four-point support of the disc in the way that

- The loading ball touches the disc shaped sample (radius  $R$ , thickness  $t$ ) on the compressive loaded side at its centre.

\* Corresponding author.

E-mail address: [isfk@unileoben.ac.at](mailto:isfk@unileoben.ac.at) (A. Börger).

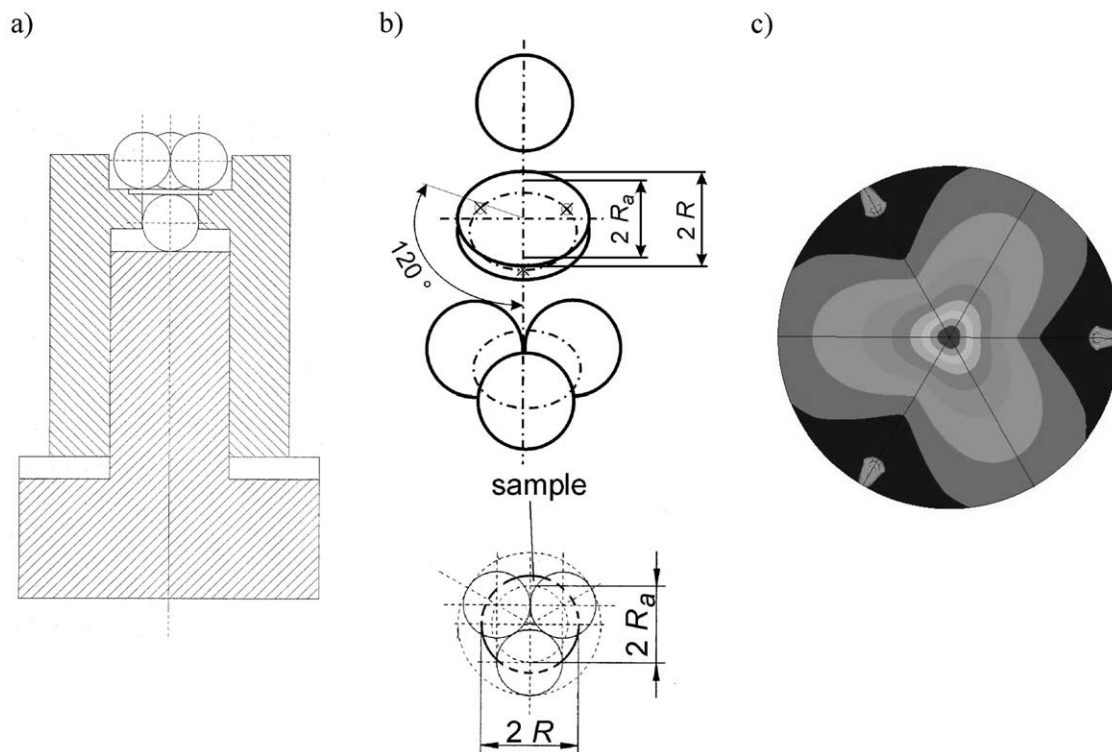


Fig. 1. (a) Experimental set-up for the ball on three balls test. Shown is a cross section of the positioning aid (the positioning aid is made of one part with concentric drillings which ensure the exact relative positioning of the disc, the loading and the three support balls relative together) which is already applied for patenting.<sup>3</sup> (b) Isometric view of the positioning of the balls relative to the sample. Marked on the sample are the contact points of the support balls. Below is a top view showing the positioning of the four balls and the sample. The three support balls (thin solid lines) touch the sample (radius  $R$ ) at the contact radius  $R_a$ . The loading ball touches the sample from the other side on its centre. (c) Example of a stress field at the tensile side of the disc for a typical loading situation (for details see Ref. 1).

- The supporting balls touch the disc on the opposite side of the disc on three points situated on a circle of radius  $R_a$ . The midpoint of the circle is the centre of the tensile loaded side of the disc where the maximum tensile stress occur. The three support points form an equally sided triangle (see also Fig. 1).

During the test the force on the loading ball is increased until fracture of the sample occurs.

The test is valid if the fracture of the sample starts at or near the centre of the tensile loaded side of the disc. This has to be assured by fractographic investigations. Relatively high tensile stresses also occur in the loading and supporting areas (Hertzian stresses). For a valid test fracture is not allowed to be caused by these stresses. As stated in the preceding paper,<sup>1</sup> the fracture patterns on the investigated materials mostly show the threefold symmetry of the fixture, but also a failing into two or four or even more large pieces can occur.<sup>2</sup> First test results are published in Ref. 4.

In the parameter range given in Table 1, the stress field in the disc specimen were analysed for the idealised configuration using the commercial FE program package ANSYS®.<sup>5</sup> Of course the maximum tensile stress occur in the centre of the disc plane opposite the loading

ball. As everywhere at the axis of the specimen, the stress state is cylinder symmetric. It has been shown, that within an accuracy of more than 1%, the maximum tensile stress amplitude,  $\sigma_{\max}$ , can be approximated by point loading (this is only true for the maximum tensile stress. To determine the stress field in the whole disc, it is necessary to model the contact area between the balls and the disc.)<sup>1</sup> It is given by the following equation:

$$\sigma_{\max} = f \cdot \frac{F}{t^2}. \quad (1)$$

$F$  is the force and  $t$  is the thickness of the disc specimen. The dimensionless factor  $f$  as a function of the disc geometry,  $t/R$ , the support geometry,  $R_a/R$  and the Poisson's ratio of the disc material,  $\nu$ , is approximated by:

Table 1  
Evaluated range of the parameters

Parameter	Evaluated range
$R_a/R$	0.55–0.9
$t/R$	0.05–0.6
$\nu$	0.20–0.35

$$f\left(\frac{t}{R}, \frac{R_a}{R}, \nu\right) = c_0 + \frac{\left(c_1 + c_2 \frac{t}{R} + c_3 \left(\frac{t}{R}\right)^2 + c_4 \left(\frac{t}{R}\right)^3\right)}{1 + c_5 \frac{t}{R}} \times \left(1 + c_6 \frac{R_a}{R}\right). \quad (2)$$

The parameters for  $c_0$  to  $c_6$  depend on the Poisson's ratio (Table 2). These results are valid for the evaluated parameter range given in Table 1.

It is interesting to note, that, in the parameter range investigated, the maximum tensile stress ( $\sigma_{\max}$ ) is determined to a large extend by the applied force,  $F$ , and the thickness,  $t$ , of the specimen. The other parameters have only little influence on  $\sigma_{\max}$ . Their influence is expressed in the factor  $f$ . In the range of parameters investigated the smallest value of  $f$  is 0.95 ( $\nu=0.2$ ,  $t/R=0.60$  and  $R_a/R=0.55$ ) and the highest value is 3.0 ( $\nu=0.35$ ,  $t/R=0.05$  and  $R_a/R=0.9$ ). The factor  $f$  increases with increasing thickness of the disc ( $t/R$ ; in the range of parameters investigated up to a factor 2.1), with increasing ratio  $R_a/R$  (decreasing overhang of the specimen over the support; it increases up to a factor 1.5) and with increasing Poisson's ratio of the disc material ( $\nu$ ; up to a factor 1.2). The influence of all other parameters on the factor  $f$  is negligible (less than 1%) [for the case of a loading ball with a larger diameter as the supporting balls (up to a factor of 2 here) a further numerical analysis shows, that, in the parameter range investigated (Table 1) the maximum tensile stress,  $\sigma_{\max}$ , remains almost constant (the changes are smaller than 1%).]

The above mentioned results were calculated using idealised testing circumstances and idealised geometric conditions. In the following parts of this paper different possible sources of errors which can lead to deviations from these idealised conditions are discussed.

Since the solution for the maximum tensile stress has an accuracy of 1% errors much smaller than 1% will be assumed to be negligible.

Table 2  
Calculated values for the dimensionless constants  $c_i$  used in Eq. (2) for four different Poisson's ratios

	$\nu = 0.2$	$\nu = 0.25$	$\nu = 0.3$	$\nu = 0.35$
$c_0$	−12.354	−14.671	−17.346	−20.859
$c_1$	15.549	17.988	20.774	24.403
$c_2$	489.2	567.22	622.62	716.41
$c_3$	−78.707	−80.945	−76.879	−76.16
$c_4$	52.216	53.486	50.383	49.615
$c_5$	36.554	36.01	33.736	32.555
$c_6$	0.082	0.0709	0.0613	0.0523

## 2. The influence of friction

It is well known for bending tests that the friction between support and specimen can be of great significance for the determination of the stresses in the specimens.<sup>6,7</sup> Similar effects may also be expected for the B3B-test. In order to investigate the frictional effects further, the contact situation and especially any possible relative movement between the balls and the disc has to be observed closer.

The analysis was performed in analogy to the calculations described in the preceding paper<sup>1</sup> using the FEM package ANSYS® (Rel. 7.0). It is assumed that the test assembly maintains its three-fold and mirror symmetry during the test. Therefore only a sixth of the whole system has to be modelled. The movement of any point in the symmetry plane of the disc and the loading ball is only possible in planes, which contain the axle of the system. Of course system points on the axle can only move in the direction of the axle. For sake of simplicity it is further assumed that the deformation of the balls is symmetrical with respect to the plane perpendicular to the axle and through the midpoint of any ball (this doesn't hinder a rolling of the balls). Therefore only a half of each ball has to be modelled. Eight node brick elements were used to model disc and balls. At and around the contact areas between disc and balls the surfaces are modelled by surface contact elements. The FE model, which consists of approximately 100.000 elements, is shown in Fig. 2. It should be kept in mind,

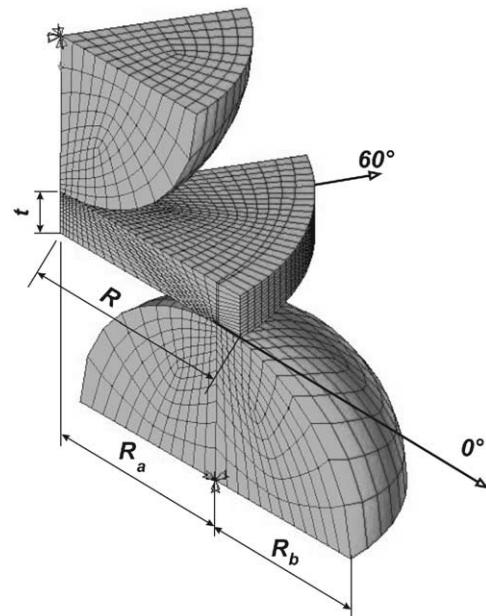


Fig. 2. FE-model of the ball on three balls test assembly: the midpoint of the centred loading ball is only allowed to move vertically; the radii of the supporting balls and of the loading ball are chosen to be equal.

that the analysis of model cases for friction will require additional model depending boundary conditions.

The friction analysis is non-linear, because the contact geometry (i.e. the contact area or the mean contact distance) of the system changes non-linearly with the applied load (or with  $\sigma_{\max}$ ). Therefore, the analysis has to be conducted at several loads levels. If not mentioned otherwise the calculations are made using the parameters (standard model) given in Table 3.

It has been shown in a preceding paper,<sup>1</sup> that—in the range of interest— $\sigma_{\max}$  does not depend on the elastic properties of the fixture material and also not on the Young's modulus of the investigated material. This is not necessarily true if friction is taken into account. Possible materials for the fixture are steel (the cheapest solution), hard metal or high strength ceramics (e.g. alumina, silicon carbide or silicon nitride). For the standard model the properties of steel were used because it is very likely that fixtures will be made from the cheapest material. The other possible fixture materials are stiffer and therefore, the influence of friction is less pronounced. Examples for that behaviour will be given in the following subchapter. Therefore the steel fixture gives an upper bond for frictional effects. Ashby<sup>8</sup> reports values of  $\mu = 0.1$ – $0.5$  for steel on ceramics and  $\mu = 0.05$ – $0.5$  for ceramics on ceramics. Therefore the used value of  $\mu = 0.5$  gives an upper limit for frictional effects. Examples for the influence of the other parameters in Table 3 on the frictional behaviour of our specimens will be discussed in this chapter.

In the B3B test assembly two types of contact pairs, the first one on the loading ball, and the second on the supporting balls, exist. For the contact pair loading ball and disc, no relative movement between the central contact point at the ball and that of the disc is possible for reasons of symmetry. The only source of frictional stresses is therefore the difference in the strains in the disc and the ball surface (parallel to the contact area). It follows from the numerical analysis of extreme geometrical and loading situations that for this contact pair the frictional stresses have almost no influence on  $\sigma_{\max}$  (the changes in  $\sigma_{\max}$  are much smaller than  $10^{-3}$  of its value). Therefore, this contact pair will be neglected in the further analysis. The second type of contact pair is more relevant and its influence will be analysed in the following for several extreme model situations.

### 2.1. Fixed supporting balls

The B3B-test can easily be realised with balls, which are fixed (glued, soldered, ...) in their position. In such a fixture sticking and sliding friction may occur. Compared with the situation with freely moving balls, the fixed ball model will yield higher frictional stresses and is therefore a worst case situation. From a mathematical point of view this model can be realised by fixing the midpoint of the supporting balls in their original position and to suppress any rotation of the balls around their midpoints.

In the support the disc is bend over the supporting balls. This causes three contributions to changes in the stress amplitude: (i) The bending shifts the mean supporting point on the ball inwards, which reduces the bending moment (for very thin specimens where strains are negligible). Therefore the point load model (Eq. 1) overestimates the maximum tensile stress. (ii) Due to the bending of the disc of finite thickness the tensile surface contacting the supporting balls is stretched. The fixed balls constrain the stretching which leads to additional compressive stresses. Again these contributions cause an overestimation of tensile stresses by the point load model. (iii) Furthermore, due to a possible mismatch between the deformations, there also exist some differences in the surface strains between disc and balls. As discussed before this mismatch is very small and in this case also far away from the maximum tensile stress amplitude. These three effects superpose and are accounted for in the following calculations. In Fig. 3, the difference between the solution of the model accounting for the friction as discussed above and the solution of the frictionless point load model is plotted in relative units. Plotted are results for the standard model (bold line, see also Table 3) and for specimens with a higher elastic modulus.

The relative influence of friction on the determination of the tensile stresses increases with the applied load. As expected the influence of sliding friction is much more relevant for materials with a low as with a high modulus. In the case of the material with a modulus of 100 GPa, the stiffer steel balls are elastically pressed into the specimen and any relative movement between disc and balls is accompanied with a high elastic deformation energy. For these materials the influence of the friction

Table 3  
Parameters used in the standard model

Geometrical parameters of specimen and support	$R = 10 \text{ mm}$ , $t = 2 \text{ mm}$ , $R_a = 8.7 \text{ mm}$
Elastic properties of the specimen	$\nu = 0.30$ , $E = 100 \text{ GPa}$
Elastic properties of the fixture	$\nu = 0.35$ , $E = 210 \text{ GPa}$
Coefficient of friction between specimen and fixture	$\mu = 0.50$

on  $\sigma_{\max}$  steeply increases with applied load. The tensile strength of low modulus ceramic materials is, in general, very limited (around 200 MPa or less). Therefore no higher tensile stresses can be applied and the relative change of the maximum tensile stress (compared with the point load model) is smaller than  $\pm 0.7\%$ . For high modulus materials strength can be 1000 MPa or even higher. For this materials the influence of friction is smaller than 1%.

Fig. 4 shows influence of the disc thickness of the specimen (a) and of the support situation (b) on the relative change of the maximum tensile stress. For all analysed situations the same elastic properties and the same friction coefficient as in the standard model were used and only the geometry of the specimen and of the loading situation is varied. The results of the standard

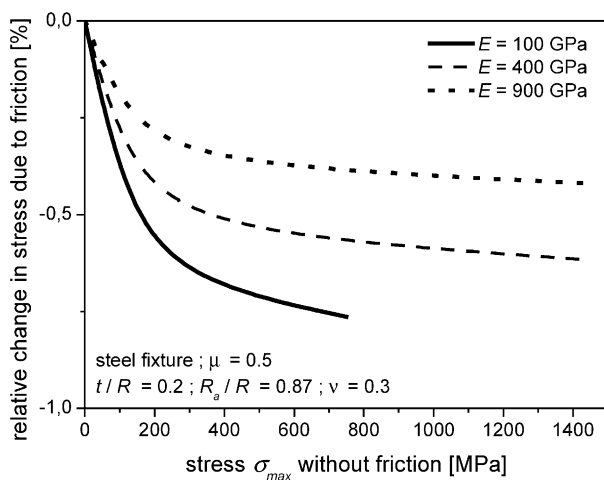


Fig. 3. Plotted is the maximum tensile stress in the sliding friction model (fixed balls) minus the maximum tensile stress calculated in the point load model without friction in relative units versus the maximum tensile stress calculated without friction. Shown are results from the standard model ( $t/R=0.2$ ,  $R_a/R=0.87$ ,  $E=100$  GPa) and additional curves for specimens with a higher modulus.

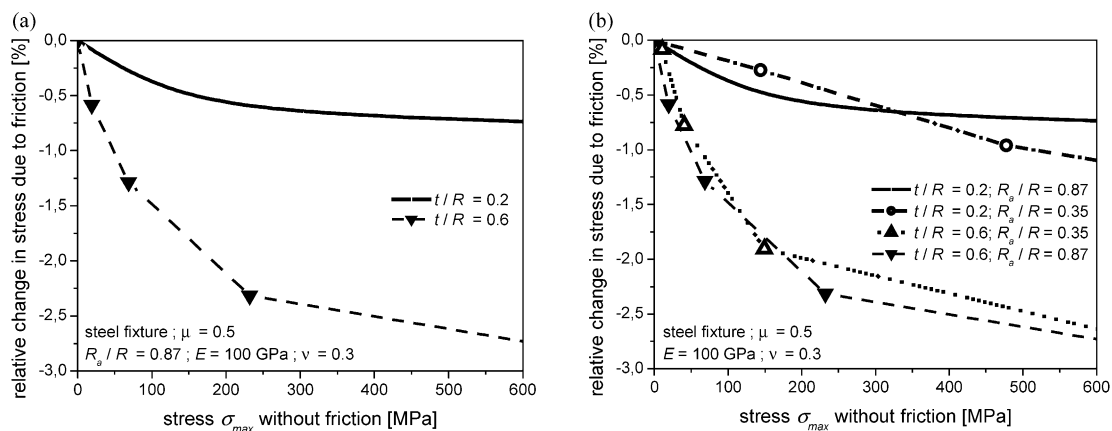


Fig. 4. Same representation as in Fig. 3 and for specimens with (a) different disc thickness ratios  $t/R$ ; (b) different support ratios  $R_a/R$  (the ratio  $t/R$  is 0.2 and 0.6 respectively).

model are shown by the bold line. Fig. 4a shows the most critical situation analysed: thick specimens and fixed supporting balls for  $R_a/R=0.87$ . For the case of  $t/R=0.6$  (the highest allowed ratio in the range of parameters, see Table 1) the relative influence of friction on the maximum tensile stresses can be higher than 1% if the applied load is high enough. For a fracture strength of 100 MPa the influence is smaller than  $\pm 1.5\%$  and for a fracture strength of around 200 MPa it is smaller than  $\pm 2.5\%$ . For a support situation with  $R_a/R=0.35$  (Fig. 4b) the situation is quite similar.

To summarise the results it can be stated, that in the parameter range investigated and for a support with fixed balls, friction will always lead to a decrease of  $\sigma_{\max}$  in the disc (i.e. an overestimation of the stress by the point load model). The effect is the higher the higher the strength and the higher the ratio thickness to radius of the specimen is. The influence of the support radius  $R_a/R$  on the friction is much less pronounced. The highest influence of friction on the maximum tensile stress in the discs occurs—in the parameter range investigated—in low modulus materials having a strength determined in specimens with  $t/R=0.6$ . This influence can reach—in extreme situations—some percent of the determined value. In general it will be less or much less than  $\pm 1\%$ .

## 2.2. Free rolling supporting balls

It is assumed, that the three supporting balls touch each other to form an equally sided triangle at the start of the test. Furthermore at the contact between the balls and the disc sticking friction and traction free rolling of the balls itself is assumed. A ball can only roll in the inward direction, if its positioning was not accurate, i.e. if the balls did not touch. Anyway, as shown in the former chapter, there will only be forces which try to roll the balls outwards.

Two cases with the free rolling balls were studied:



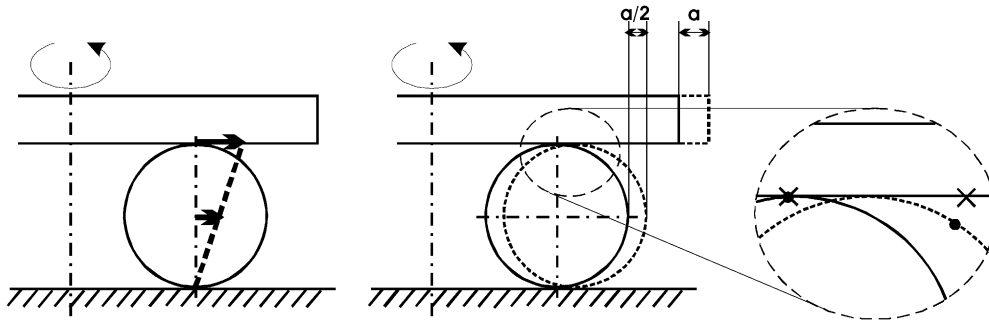


Fig. 5. Geometric behaviour of a free rolling ball. The outwards shift of the midpoint of the support ball is half the shift of the contact point to the disc.

1. The support balls are allowed to rotate around their centre. This means that the balls instantly follow any forces trying to rotate it, but the actual position of the balls (i.e. their midpoints) does not change. In this case the only change to the point load model is the inward shift of the contact point due to the bending of the specimen.
2. The ball can rotate and also move outwards. As shown in Fig. 5 the shift of the centres of the supporting balls is the half of the shift of their contact points to the specimen. Additional stresses occur due to the rolling friction (it should be noted that the rolling friction coefficient depends to a large extent on the surface condition of the analysed materials. In general it is much smaller than the sticking or sliding friction coefficient, therefore it is neglected in the model.) They are much less pronounced than stresses due to sticking or sliding friction. In addition the initial support points move outwards, increasing the support radius and the bending moments. Numerical calculations on extreme situations show that, in the case of free rolling supporting balls, the influence of friction on the tensile stresses is much less pronounced (at least one order of magnitude) as in the case of fixed supporting balls. Therefore friction can be neglected in all analysed cases.

### 2.3. Contact forces between the supporting balls

A compressive load on the supporting rolls will cause an enlargement of the equator of the balls. If the balls touch each other, this will cause contact forces between the supporting balls, which will force the balls to move in outward direction. The balls can slip (i) or roll (ii), depending whether the frictional forces in the contact areas between disc and ball and between ball and support are similar or quite different. This effect will cause additional tensile stresses in the tensile plane of the

specimen which are not accounted for in the point load model.

In the FE model, the first case (i) can be described by introducing additional contact elements in the plane between two neighbouring supporting balls. The numerical calculations show that this effect is much less important than the influence of the frictional forces between the support balls and the disc discussed above. The second case (ii) is quite equal to the case discussed in Chapter 2.2. Only the absolute movement of the balls is even smaller hence causing less frictional effects.

In summary, contact forces between supporting balls have a very weak influence on the maximum tensile stresses (much less than  $10^{-3}$  of  $\sigma_{\max}$ ) and therefore they can be neglected.

### 3. Buckling of the disc

The ideal geometry of the test assembly has a three-fold symmetry and the deflection of the disc shows it also in the case of small deflections. But even if the balls are positioned accurately, there exists a further meta-stable deflection of the disc for larger deflections, which shows a double symmetry. Examples for the deflection of the disc with threefold and twofold geometry are shown in Fig. 6a and b, respectively. In principle buckling of the disc can occur from the threefold to the twofold symmetry state. To investigate this possibility a buckling analysis was performed. Details on the approach for a buckling analysis can be found in (Ref. 9). The calculations were made for a point support which is the worst case assumption.

The analysis showed that in the parameter range investigated (Table 1) and for small deflections ( $< 2 \cdot 10^{-2}$ ) buckling is extremely unlikely to occur. In ceramic materials the deflections are always small ( $< 2 \cdot 10^{-3}$ ) and buckling is not possible in the parameter range investigated (it is only possible for very thin discs and large deflections).

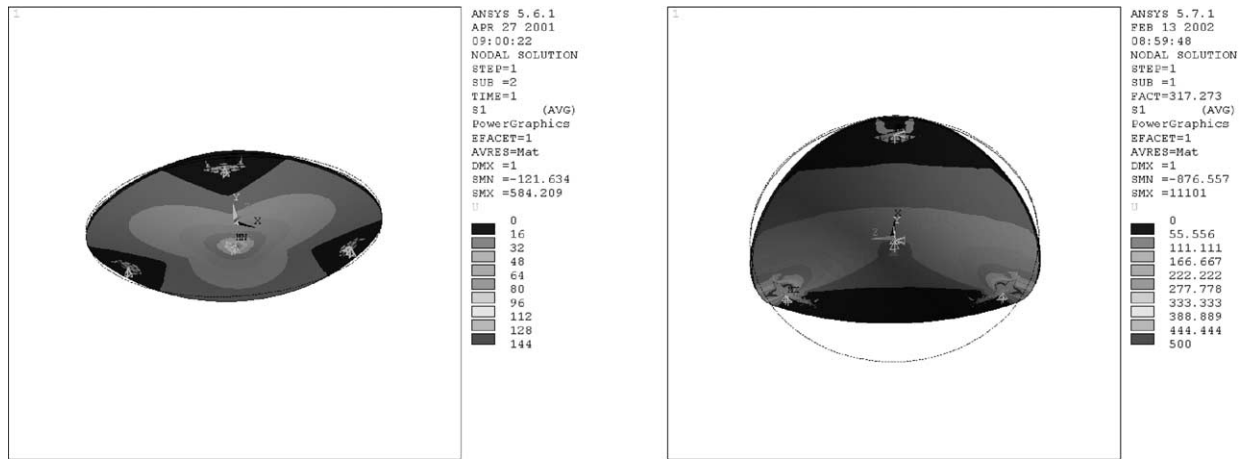


Fig. 6. Thin deformed discs with a point support with  $R_a/R=0.87$ . Shown is a deflection: (a) with a threefold symmetry, which is stable for small deflections (b) with a double symmetry, which is stable for large deflections.

#### 4. Force measurement, geometric imperfections, material parameter uncertainty

Following Eq. (1) the maximum tensile stress in the disc depends on three factors:  $\sigma_{\max} = F \cdot (1/t^2) \cdot f$ . In the following the influence of the uncertainty of the determination of these factors on the accuracy of the determination of the maximum stress is discussed.

The first factor in the upper equation is the force,  $F$ . It is only limited by the uncertainty of the load cell of the testing machine. If an adequate load cell is used the force can be measured with an accuracy far better than  $\pm 1\%$ . As the stress scales linearly with the force this effect can be neglected.

The second factor, can be developed in a Taylor series which can be interrupted after the first order term:  $1/t^2 \sim [1/(t_0)^2] \cdot (1 - 2\Delta t/t_0)$ , with  $(t - t_0) = \Delta t$ , ( $t$ : real thickness of the disc,  $t_0$ : measured thickness of the disc). For disc specimens with flat and parallel bottom and top planes, see Fig. 7a), the thickness of the disc can easily be determined using a micrometer screw with an accuracy of much better than  $\pm 5 \mu\text{m}$ . If the specimen is thicker than  $500 \mu\text{m}$ , the corresponding measuring error of the thickness is smaller than  $\pm 1\%$  and that of the maximum tensile stress is smaller than  $\pm 2\%$ .

For specimens with deviations of the ideal shape of a disc as shown in Fig. 7b–e (wedge shaped specimens,

buckled specimens and so on) the determination of a single thickness value may be not meaningful (case b and c) or the measurement can be very inaccurate (case d and e). This aspect may be of importance when testing ceramic discs in the as sintered condition. In general there is a tendency to overestimate the thickness of the disc. This problem is discussed in more detail in the following. The most common imperfect geometries of discs found during tests are samples according to Fig. 7b and a double convex geometry. These two geometries were modelled and investigated in detail.

##### 4.1. Inclination of the disc (top and bottom surfaces are not parallel)

The geometry used in the model calculation is shown in Fig. 8. The thickness in the disc centre is kept to be the reference value,  $t$ . The thickness at the distance  $R$  from the centre has a maximum value,  $t_1$ , and a minimum value,  $t_2$ , according to the inclination angle,  $\theta$ , which was used as a parameter in the model.

There are several possibilities for the positioning of the support balls relative to the maximum and minimum thickness of the disc. Three possible cases for these positions were modelled and will be referred to in the following as case I, case II and case III as shown in

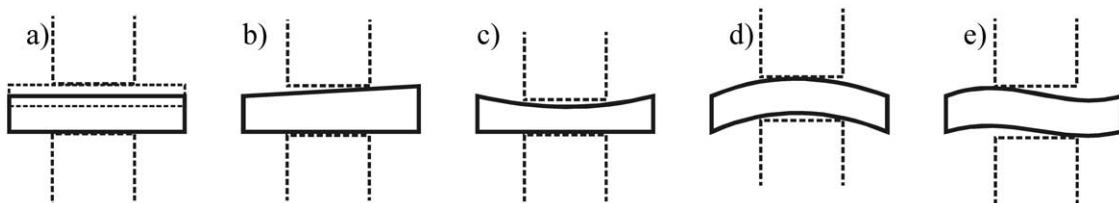


Fig. 7. Overview of some common errors in measuring the disc thickness. The two dashed cylinders are the measurement cylinders of a caliper. (a) Absolute error in measurement by inaccurate measuring device or inaccurate read off of the result. (b) Ramped disc thickness. (c) Out of flatness of the disc. (d) Bending of the disc. (e) Double bending of the disc.

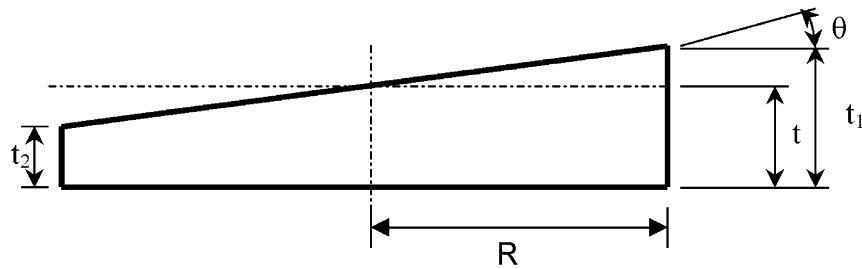


Fig. 8. Geometry for the disc with non-parallel top and bottom surface planes. The thickness in the centre of the disc,  $t$ , and the angle  $\theta$  are the first parameters for the simulation.

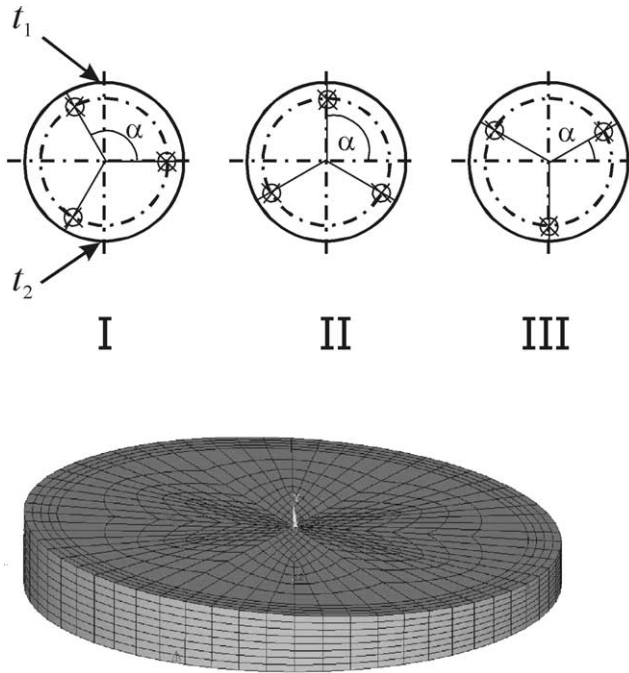


Fig. 9. Geometry for the disc with non-parallel top and bottom surface planes. Shown are the investigated cases I, II and III with different positions of the support balls relative to the maximum ( $t_1$ ) and minimum ( $t_2$ ) thickness of the disc. The thickness in the centre of the disc,  $t$ , and the angle  $\theta$  are the first parameters for the simulation. Furthermore an isometric view of the mesh on an inclined disc is shown.

Fig. 9a–c. The angle  $\alpha$  to the first ball was used as a third parameter. As can be seen in Fig. 9 the symmetry of the model is widely lost which requires a full 360° 3D modeling of the disc. Of course this also leads to a loss of symmetry in the resulting stress field in the disc which will have a significant influence on the effective loaded volume.

According to Fig. 10 the three cases give almost the same error for inclination angles  $< 3^\circ$ . For an error in the maximum tensile stress of less than  $\pm 1\%$  the inclination must not exceed  $\pm 1^\circ$ . For a disc with standard geometry ( $R_a/R = 0.87$ ,  $t/R = 0.2$ ) this condition allows a difference between the maximum and minimum thickness of 16% (for a 2 mm thick disc this are 320  $\mu\text{m}$ ).

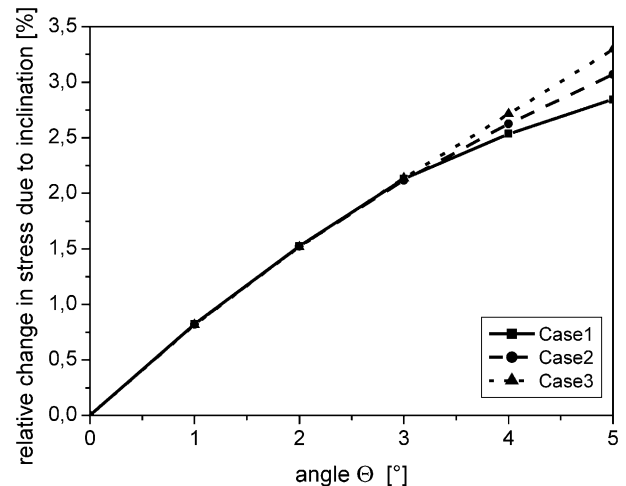


Fig. 10. Relative error in the maximum tensile stress as a function of the inclination angle of the disc. Again the geometry and material parameters of the standard model were used.

This condition can easily be fulfilled if the specimens are grinded. It should be kept in mind that for the test evaluation the thickness should be determined in the centre of the specimen.

#### 4.2. Convex disc geometry

Another shape possible for as sintered specimens is the double-convex geometry as shown in Fig. 11. Again for comparisons the thickness at the centre of the disc is kept to be the reference thickness,  $t$ , and the thickness at the circumferential of the disc,  $t_1 = t - 2H$ , is different. For definitions see Fig. 11. The top and bottom planes of the disc are assumed to be spherical callots.

In Fig. 12 the relative error in the maximum tensile stress is plotted versus the relative change in the thickness due to the curvature of the disc. For a maximum error in the maximum tensile stress of  $\pm 1\%$ , a relative difference in the thickness between the centre of the disc and its circumference of  $\pm 5\%$  can be tolerated. As discussed in Section 4.1 the thickness in the centre of the disc is of most relevance and again it is suggested to use the thickness in the centre of the disc for data evaluation. The thickness at the circumference should only



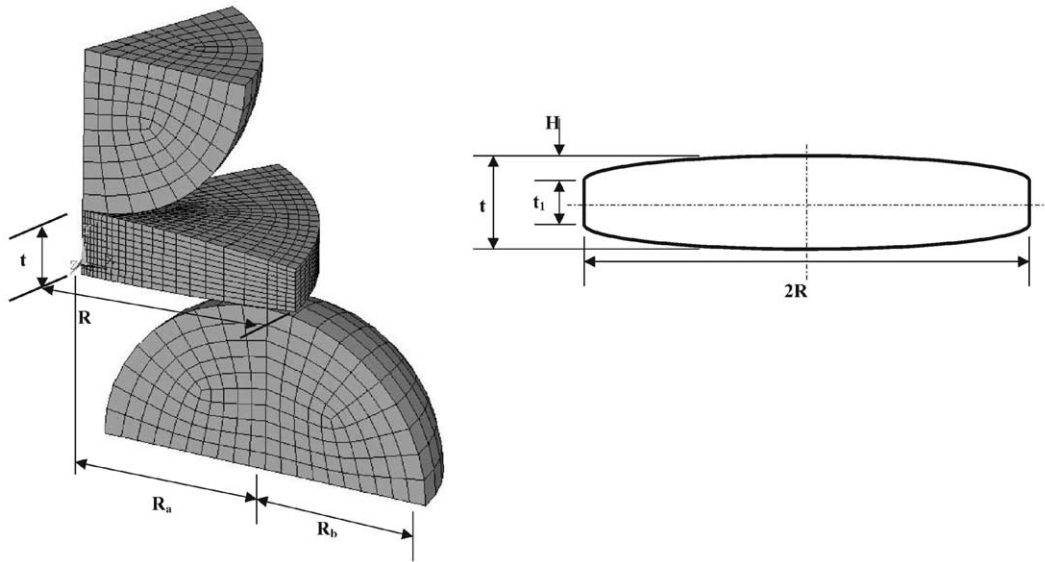


Fig. 11. Double convex geometry of the specimen. Plotted is the mesh of a sixth of the model, which can be used for symmetry reasons, and below a cross section of the disc showing the shape and the maximum and minimum thickness.

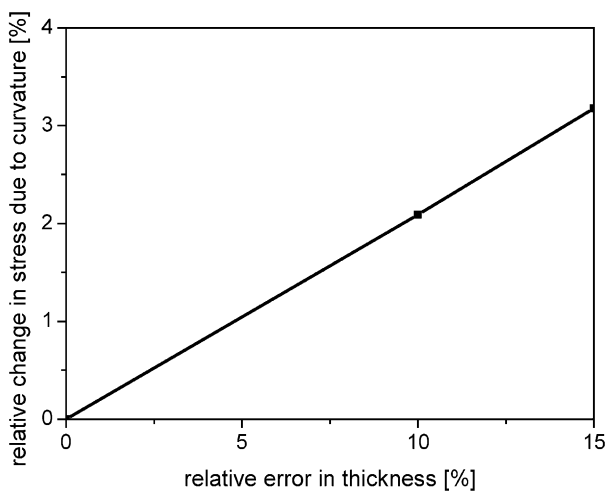


Fig. 12. Relative error in the maximum tensile stress as a function of the relative error in the disc thickness  $100(t-t_1)/t$  between the disc centre and its circumference. Again the geometry and material parameters of the standard model were used.

be checked to decide whether the above condition is fulfilled or not.

#### 4.3. The influence of the factor $f$

The last factor, the function  $f$ , depends on the geometric parameters  $t/R$ ,  $R_a/R$  and on the material parameter  $\nu$ . The variation of the factor  $f$  on measurement inaccuracies of the parameters  $R$ ,  $R_a$  and  $t$  and  $\nu$  can easily be derived from Eq. (2). Of course for small inaccuracies  $\Delta x$  ( $x = R$ ,  $R_a$ ,  $t$  or  $\nu$  the error in the stress linearly depends on  $\Delta x$  as shown in Fig. 13. The influence of small variations of these parameters ( $\Delta x$ ) on  $f$  is

very small. In the investigated range it holds:  $|\Delta f| < |0.4 \cdot \Delta x|$ .

In principle the accuracy of the measurement of the disc radius (measured using a micrometer screw) or thickness is much better than  $\pm 10 \mu\text{m}$ . Therefore for any measured length higher than  $500 \mu\text{m}$  the corresponding measuring error is less than  $\pm 1\%$ .

The determination of the support radius is via the measurement of the diameter of the balls and of the diameter of the positioning aid. The three balls should fit perfectly into the hole of the positioning aid (see Fig. 1). To keep the measuring error below  $\pm 1\%$  and for a specimen with a support radius  $R_a$  of  $0.8 \text{ mm}$  a gap of  $30 \mu\text{m}$  between the balls is tolerable. This can be ascertained by measuring the diameter of the balls using a micrometer screw.

For many ceramic materials the Poisson ratio,  $\nu$ , is not precisely known. Most of the reported data are between  $\nu = 0.2$  and  $\nu = 0.3$ . It follows from the above analysis (Fig. 13) that for an error of  $\Delta \nu = \pm 0.05$  the possible error in  $\sigma_{\text{max}}$  is smaller than  $\pm 5\%$ .

#### 4.4. The influence of other geometrical imperfections

It is a consequence of the deflection of the disc, that the contact point between the disc and the support ball will move and therefore the support radius of the disc changes. This is a geometric effect caused by the curvature of the balls. This effect can be treated in the same way as the effect of an inaccurate measurement of the support radius, see Fig. 13. The consequences for the determination of  $\sigma_{\text{max}}$  can be neglected.

Finally deviations from the idealised geometry used for the numerical analysis may arise due to an imperfect

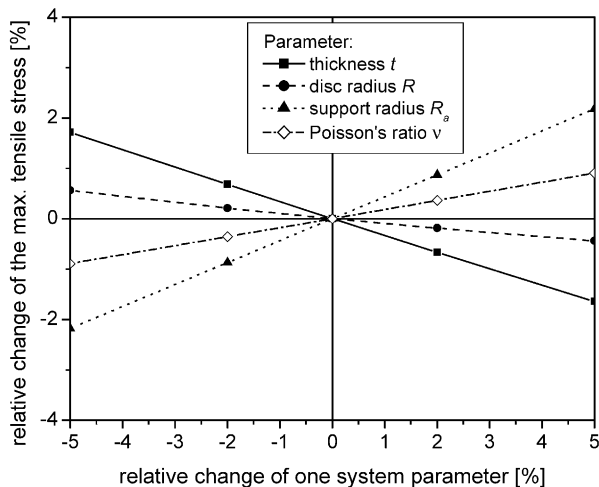


Fig. 13. Relative change in the calculated maximum tensile stress in the disc in % if the parameters  $t$ ,  $R$ ,  $R_a$  and  $\nu$  are inaccurate. The most significant influence on the stress values is caused by the thickness  $t$ . The stress values were calculated for assumed correct values for  $t=2$  mm,  $R=10$  mm,  $R_a=7$  mm and  $\nu=0.25$ . Nevertheless a change of this starting values does not change the results of the error in the calculated maximum tensile stress if the same relative errors in the parameters are used.

positioning of the balls or the disc. Three different possibilities have to be considered:

- excentric positioning of the loading ball relative to the support balls;
- excentric positioning of one or more of the supporting balls relative to the loading ball and the disc; and
- excentric positioning of the disc relative to the balls.

If the loading ball is excentric the distance to at least one support ball increases and to at least one other support ball decreases. These changes can be limited using the smaller and the higher distance for calculating lower and upper bonds of the support radius  $R_a$ . The corresponding bonds for the maximum tensile stress can be read off Fig. 13. For a support radius of several millimetres and for  $R_a \pm 0.1$  mm the error in determining  $\sigma_{\max}$  is smaller than 1%.

The same approach giving the same result as above can be used if one or more of the loading balls are excentric. It can be noted that in that case the support radius can only increase (not decrease) as the balls are assumed to be in touch with each other.

The last mentioned point is a non centric positioning of the disc itself. Again the consequence of this can be estimated by a simple consideration. If the disc is excentric this means that the overhang of the disc over the support balls changes. It gets smaller on one side and increases on the opposite side. This effect can be

treated by calculating lower and upper points of error in a similar way as shown before. It can be read off Fig. 13 that this possible error is negligible.

For all three cases considered above there also occurs a disturbance of the threefold symmetry of the stress field, but again this effect on the maximum tensile stress is negligible.

## 5. Discussion and summary of the results

The main advantage of the B3B test is the fact, that the loading situation (with three supporting and one loading ball) is much better defined as in the standardised ring on ring test,<sup>10</sup> where small geometric inaccuracies can cause a break of the axial symmetry of the testing assembly. This may cause big changes in the maximum tensile stress compared to the model solution. The B3B test has been developed for the strength testing of electro-ceramic materials where many components have the shape of discs. These materials fail by brittle fracture, which starts at large crack like flaws distributed in the material. The thickness to radius ratio of many resistor components is in the range from  $0.05 \leq t/R \leq 0.6$ . Therefore the stress analysis in Ref. 1 and also in this paper is restricted to this parameter range.

In (very) thin plates high tensile stresses are concentrated to a small area underneath the loading ball and the situation resembles to that of a rubber sheet punched by a needle (i.e. membrane system). The loaded volume is very small and other fracture modes as brittle fracture starting from large flaws are likely to occur. Therefore this situation is not tackled in this paper and the reported solutions are not applicable for thin plates. In the case of thin plates the ring on ring testing procedure seems to be more appropriate: The applied deflection are relatively large, which helps to accommodate small geometric inaccuracies and the volume under high tensile stresses is also much larger as in the case of the B3B test, which promotes the search for large flaws.

In the case of testing thick (compared to thin) discs the failing of the specimen caused by Hertzian cracks<sup>11</sup> starting underneath the loading ball (this is a kind of edge cracking)<sup>12</sup> gets more and more relevant. Therefore this testing procedure is also restricted to not too thick discs and the analysis of the stress fields in tested discs is restricted to the thickness to radius ratio  $0.05 \leq t/R \leq 0.6$ . The uncertainty of the numerical calculations is less than  $\pm 1\%$  of the true value within the continuum-mechanical approach. Therefore all uncertainties much less than  $\pm 1\%$  are neglected in the following.

The possible sources for uncertainties when measuring the strength of brittle discs arise from the following reasons:

- (i) uncertainties of the force measurement;
- (ii) friction between the parts of the fixture and the specimen;
- (iii) uncertainties of the determination of geometrical dimensions; and
- (iv) uncertainties of the determination of elastic properties of the material of the specimen.

ad (i): In a state of the art measurement these uncertainties are much smaller than  $\pm 1\%$  of the strength value and can, therefore, be neglected.

ad (ii): Using some extreme model assumptions friction has been found to exceed  $\pm 1\%$  of the strength value for

fixtures with fixed balls;  
specimens with a high ratio of thickness to radius; and  
materials having a low modulus and a high strength.

If one of these conditions is not valid the influence due to friction is less or much less than  $\pm 1\%$  of the strength value. Especially if fixtures with freely movable balls are used, the friction is much less than  $\pm 1\%$  of the strength value and can therefore be neglected.

ad (iii): Three geometrical parameters have influence on the determination of the strength of brittle discs: support radius, specimen radius and specimen thickness. The uncertainties in the support radius results from uncertainties of geometric properties of the measuring device and of the uncertainties in positioning of the specimen in the device. These uncertainties depend—to a large extend—from the accuracy of the manufacturing process of the fixture and the positioning aid. The precision necessary to get measurement uncertainties of less than  $\pm 1\%$  can easily be reached when testing large specimens (radius several millimetres or more) but special care is necessary when manufacturing fixtures for specimens of about millimetres or less.

For specimens with a radius of at least millimetres or more the radius can easily be determined with an accuracy high enough, that the influence of possible errors on the strength can be neglected.

The thickness of the specimen is the most relevant parameter for the determination of the strength. Its measurement uncertainty must be  $\pm 0.4\%$  or less to reduce the uncertainty in strength to  $\pm 1\%$  or less. The thickness is the smallest geometrical property to be measured and it is also the worst defined property. For precisely machined specimens having a thickness of around  $500\text{ }\mu\text{m}$  the accuracy of the measurement should be  $\pm 2\text{ }\mu\text{m}$ . In principle such a precise measurement is possible with a precision micrometer screw. For thinner

specimens the necessary accuracy can hardly be reached. For specimens with several millimetres thickness, the requirement can easily be fulfilled with standard measurement equipment.

It should be kept in mind that the B3B test has also been designed to test as sintered specimens without any machining. In this case, the shape of the specimen can deviate from that of a disc. Again the thickness is the property which has to be determined with the highest accuracy. If the thickness is not constant, the thickness in the centre of the disc has to be used for the determination of strength. Of course the deviations of the disc shape from the model shape should not be too large.

ad (iv): Data for the Poisson ratio can hardly be found in the literature and an absolute accuracy of  $\pm 0.05$  results in relative accuracy of 25%, assuming a value  $\nu = 0.2$ . Such a large uncertainty would cause a uncertainty in the strength of about 5%. To reduce the uncertainty in strength to  $\pm 1\%$  the Poisson ratio has to be known with an uncertainty of about 0.01 or less. This may be the limiting factor in the precise determination of strength using the B3B test.

## 6. Conclusions

- The error analysis shows, that the B3B test is very tolerant against possible errors with respect to the alignment of specimens, the determination of the supporting radius or the measurement of the radius of the specimen.
- If a support with freely moving balls is realised the influence of friction on the data evaluation can be neglected.
- Very important for the data evaluation is the accurate determination of the thickness of the disc, which may be a limiting factor for a possible miniaturisation of the specimen. From that a lower limit for the disc thickness is  $500\text{ }\mu\text{m}$ , if measurements uncertainties of less than  $\pm 1\%$  of the strength value are required (the thickness can be as small as  $100\text{ }\mu\text{m}$ , if uncertainties of  $\pm 5\%$  can be tolerated.)
- A second limiting factor for the reduction of the uncertainties is the requirement, that for a proper data evaluation, the Poisson ratio of the tested material has to be known with an accuracy of  $\pm 5\%$  (to limit uncertainties in strength to  $\pm 1\%$ ) or to  $\pm 25\%$  (to limit uncertainties in strength to  $\pm 5\%$ ), what is not the case for any material.
- If as sintered ceramics are tested, the thickness of the disc has to be determined in the centre of the disc.

## References

1. Börger, A., Supancic, P. and Danzer, R., The ball on three balls test for strength testing of brittle discs—stress distribution in the disc. *J. Eur. Ceram. Soc.*, 2002, **22**(8), 1425–1436.
2. Morrell, R. et al., Biaxial disc flexure-modulus and strength testing. *Brit. Ceram. Trans.*, 1999, **98**, 234–240.
3. Leoben, M. C. L., Danzer, R. et al. *Methode und Vorrichtung zur Prüfung von Scheiben*. 2002, Applied for Patent, A 738/2002-1, Austria.
4. Danzer, R. et al., Ein einfacher Festigkeitsversuch für Scheiben aus spröden Werkstoffen. *Mat.-wiss. u. Werkstofftech*, 2003, **34**, 490–498.
5. ANSYS 7.0, Copyright® 2002 SAS IP.
6. Lube, T., Manner, M. and Danzer, R., The miniaturisation of the 4-point bend-test. *Fatigue Fract. Engng. Mater. Struct.*, 1997, **20**(11), 1605–1616.
7. Baratta, F. I., Matthews, W. T. and Quinn, G. D., *Report MTL TR 87-35*. US Army Materials Technology, Watertown, 1987.
8. Ashby, M. F., *Materials Selection in Mechanical Design*, 2nd edn. 1999. Butterworth-Heinemann.
9. Timoshenko, S. P. and Woinowsky-Krieger, S., *Theory of Plates and Shells*, 2nd edn.. McGraw-Hill International Editions, New York, 1959.
10. *Implants for Surgery—Ceramic Materials Based on High Purity Alumina*. Patent ISO 6474, 1994.
11. Munz, D. and Fett, T., *Ceramics: Mechanical Properties, Failure Behaviour, Materials Selection*. In *Materials Science*, ed. R. Hull. Springer-Verlag, Berlin, 1999.
12. Danzer, R., Hangl, M. and Paar, R., Edge Chipping of Brittle Materials. In *Fractography of Glasses and Ceramics IV*, ed. J. R. Varner, G. D. Quinn and V. D. Fréchet. The American Ceramic Society, Westerville, 2001, pp. 43–55.